



Article scientifique

Article

2006

Published version

Open Access

This is the published version of the publication, made available in accordance with the publisher's policy.

---

## Two cell wall associated peroxidases from Arabidopsis influence root elongation

---

Passardi, Filippo; Tognolli, Michael; De Meyer-Fague, Mireille Anne; Penel, Claude; Dunand, Christophe

### How to cite

PASSARDI, Filippo et al. Two cell wall associated peroxidases from Arabidopsis influence root elongation. In: Planta, 2006, vol. 223, n° 5, p. 965–974. doi: 10.1007/s00425-005-0153-4

This publication URL: <https://archive-ouverte.unige.ch/unige:118384>

Publication DOI: [10.1007/s00425-005-0153-4](https://doi.org/10.1007/s00425-005-0153-4)

Filippo Passardi · Michael Tognolli · Mireille De Meyer  
Claude Penel · Christophe Dunand

## Two cell wall associated peroxidases from *Arabidopsis* influence root elongation

Received: 9 June 2005 / Accepted: 19 September 2005 / Published online: 12 November 2005  
© Springer-Verlag 2005

**Abstract** Two class III peroxidases from *Arabidopsis*, AtPrx33 and Atprx34, have been studied in this paper. Their encoding genes are mainly expressed in roots; *AtPrx33* transcripts were also found in leaves and stems. Light activates the expression of both genes in seedlings. Transformed seedlings producing AtPrx33-GFP or AtPrx34-GFP fusion proteins under the control of the CaMV 35S promoter exhibit fluorescence in the cell walls of roots, showing that the two peroxidases are localized in the apoplast, which is in line with their affinity for the Ca<sup>2+</sup>-pectate structure. The role they can play in cell wall was investigated using (1) insertion mutants that have suppressed or reduced expression of *AtPrx33* or *AtPrx34* genes, respectively, (2) a double mutant with no *AtPrx33* and a reduced level of *Atprx34* transcripts, (3) a mutant overexpressing *AtPrx34* under the control of the CaMV 35S promoter. The major phenotypic consequences of these genetic manipulations were observed on the variation of the length of seedling roots. Seedlings lacking *AtPrx33* transcripts have shorter roots than the wild-type controls and roots are still shorter in the double mutant. Seedlings overexpressing *AtPrx34* exhibit significantly longer roots. These modifications of root length are accompanied by corresponding changes of cell length. The results suggest that AtPrx33 and Atprx34, two highly homologous *Arabidopsis* peroxidases, are involved in the reactions that promote cell elongation and that this occurs most likely within cell walls.

**Keywords** Cell wall · Green fluorescent protein · Pectin · Peroxidase · Root elongation

**Abbreviations** CaMV 35S: Cauliflower mosaic virus 35S promoter · CTPP: C-terminal propeptide · DAPI: 4',6-diamidino-2-phenylindole · GFP: green fluorescent protein · ROS: reactive oxygen species · RT-PCR: reverse-transcriptase polymerase chain reaction · WAK: wall associated kinase

### Introduction

The plant specific heme peroxidases belong to a superfamily that contains three different classes of peroxidases (Welinder 1992): the intracellular class I (EC 1.11.1.5/.6/.11), the class II released by fungi during plant–fungi interaction (EC 1.11.1.13/.14), and the secreted class III plant peroxidases (EC 1.11.1.7).

Class III peroxidases are supposed to be involved in a broad range of processes in plants, due to their catalytic versatility and the great number of their isoforms (Passardi et al. 2005). In *Arabidopsis*, they constitute a multigenic family encoding 73 isoenzymes (Tognolli et al. 2002) implicated in diverse activities that are still poorly understood for each single peroxidase isoform. The great diversity of the promoter and intronic sequences partially explains that all kinds of internal or external stimuli regulate the gene expression. On the other hand, the large variability of the putative substrate access channel between the F and G  $\alpha$ -helices justifies the diversity of activities catalyzed (Gajhede et al. 1997). The flexibility of the regulation and the substrate specificity within this multigenic family could explain the omnipresence of the peroxidases in the plant life cycle.

AtPrx33 and AtPrx34 are two *Arabidopsis* peroxidases belonging to a cluster of five enzymes containing a putative Ca<sup>2+</sup>-pectate binding domain (Dunand et al. 2002) similar to the binding domain of APRX, an anionic peroxidase from zucchini (Carpin et al. 1999, 2001), which binds specifically to the Ca<sup>2+</sup>-pectate complex within cell walls (Carpin et al. 1999). APRX transcripts are mainly localized in the elongation zone of

F. Passardi · M. De Meyer · C. Penel · C. Dunand (✉)  
Laboratory of Plant Physiology, University of Geneva,  
Quai Ernest-Ansermet 30, 1211 Geneva 4, Switzerland  
E-mail: christophe.dunand@bota.unige.ch

M. Tognolli  
Swiss Institute of Bioinformatics Swiss-Prot Group,  
rue Michel Servet 1, 1211 Geneva 4, Switzerland

root and hypocotyl (Dunand et al. 2002). The Ca<sup>2+</sup>-pectate binding property could be important in regulating the enzyme activity and localization within the cell wall.

AtPrx33 and AtPrx34 show nearly 95% homology at the protein level, but their promoter and intronic sequences are strongly divergent (Valério et al. 2004). They can be expected to have similar activity and cellular localization, although the control of their expression and tissular localization could be different. If their cell wall localization is confirmed *in planta*, what could be their function therein and does the pectin binding play a role in this function?

The plant cell wall is a very dynamic structure, which controls both cell shape and cell elongation. Various enzymatic processes cleave and reassemble the cell wall constituents during cell extension. Changes in the cell wall architecture can be achieved by class III peroxidases through their two catalytic cycles: peroxidative and hydroxylic (Passardi et al. 2004). They can stop elongation by forming bonds within the cell wall or favor it by regulating the local concentration of H<sub>2</sub>O<sub>2</sub> or by generating reactive oxygen species (ROS), which breaks cell wall bonds (Passardi et al. 2004). Indirectly, peroxidases can also control the cell elongation through their auxin oxidase activity. IAA can be oxidized by following two separate mechanisms: a conventional hydrogen-peroxide-dependent pathway and a second one, which is hydrogen-peroxide-independent and requires oxygen (Savitsky et al. 1999). By this way, peroxidases might regulate locally auxin concentration. In parallel, peroxidase expression levels are dependent on the endogenous auxin concentrations (Gaspar et al. 1996).

In this work, we have combined two different approaches: the RNA silencing technique and the use of T-DNA insertion mutants to get an insight into the function of AtPrx33 and AtPrx34. The growth of seedlings lacking *AtPrx33* or *AtPrx34* transcripts was studied. In addition, the localization of the enzymes fused to the green fluorescent protein was analyzed.

## Materials and methods

### Plant material and growth conditions

The Columbia (Col) and Wassilewskija (Ws) ecotypes of *Arabidopsis thaliana* were used as wild-type controls. Plants were grown in soil or on ½ MS medium (Murashige and Skoog 1962) at 24°C under 16 h light/8 h dark and 60% humidity. For the *in vitro* culture, the light intensity was strictly controlled and fixed at 120 μmol photons m<sup>-2</sup> s<sup>-1</sup>. The T-DNA lines CS10885 mutated for *AtPrx33* (in Ws background) and SALK\_051769 mutated for *AtPrx34* (in Col background) were isolated from the Feldmann collection (Feldmann et al. 1991) and from the SALK T-DNA insertion lines (Alonso et al. 2003), respectively. All seed

lines are available from the stock center of TAIR (<http://www.arabidopsis.org>).

### Mutant screening

The collection of T-DNA insertion mutants from K. Feldmann (Feldmann et al. 1991) was screened by PCR using the *AtPrx33* sense primer 5'-ATGC AATTCTCTTCATCTTC-3', in combination with the T-DNA-specific primer CD5LB 5'-ATGCAATCGA TAT CAGCAGCCAATTTTA- 3'.

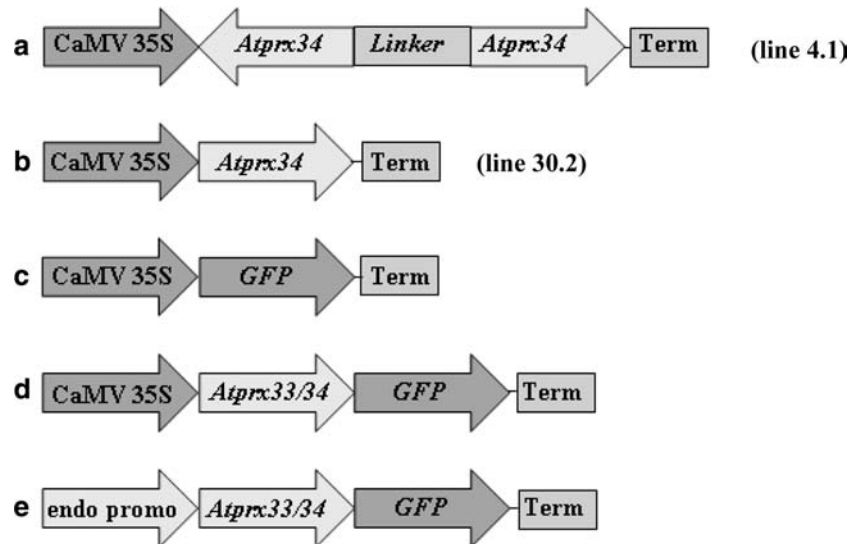
A search in the TAIR database (<http://www.arabidopsis.org>) revealed a T-DNA insertion within the promoter region of *AtPrx34* (SALK\_051769). The precise location of the insert was determined by DNA sequence analysis of a PCR amplification product that was obtained with the *AtPrx34* reverse primer 5'-TCCAAGTGGACGATGTTGAAG-3' and the T-DNA right border primer CD5RB 5'-GCTCAGGATCC-GATTGTCGTTTCCCGCCTT-3'. PCR amplification was carried out with 0.2 mM dNTPs, 0.4 μM of each primer, 10× *Taq* buffer, and 1 unit of *Taq* polymerase (Sigma) in a volume of 20 μl. The amplification program consisted of an initial denaturation at 95°C for 1 min followed by 35–40 cycles of denaturation at 94°C for 1 min, annealing at 55°C for 1 min, polymerization at 72°C for 90 s, and a final extension at 72°C for 10 min.

Homozygous insertion mutants in *AtPrx33* and *AtPrx34* were identified by PCR amplification with gene-specific primers (sense primer for *AtPrx33* and reverse primer for *AtPrx34* as described above and the reverse primer 5'-TGTTTGTGTGCCATC-3' and sense 5'-TTGAAAGGTCGTCGAGGAGT-3' for *AtPrx33* and *AtPrx34*, respectively).

### Imaging of GFP expression

The following constructs (Fig. 1c, d, e) have been designed with the purpose of studying the localization *in planta* of the AtPrx33 and AtPrx34 proteins and the role of the promoter sequence in this localization. *AtPrx33* and *AtPrx34* coding sequences lacking the stop codon were cloned in frame in pAVA 393 (von Arnim et al. 1998), respectively, with *KpnI/XhoI* and *NcoI/XhoI*. The *AtPrx33-GFP* and *AtPrx34-GFP* constructs were subcloned in pCHF3 binary vector with *KpnI* and *BglII*. 3.3 kb PCR fragment containing 1.2 kb of *AtPrx33* promoter sequence and the genomic sequence of *AtPrx33* was cloned with *KpnI* and *XhoI* in frame in pAVA 393. The *AtPrx33::AtPrx33-GFP-Term* construct obtained was subcloned in pZP222 (Hajdukiewicz et al. 1994) with *KpnI* and *BglII*. 3.3 kb PCR fragment containing 1 kb of *AtPrx34* promoter sequence and the genomic sequence of *AtPrx34* has been cloned with *HindIII* and *NcoI* in pAVA 393. The *AtPrx34::AtPrx34-GFP-Term* construct has been subcloned in pZP211 binary vector with *KpnI* and *PstI*.

**Fig. 1** Schematic structures of the gene cassettes. **a** CaMV 35S:: *43xrPtA-linker-AtPrx34* RNAi construct used to obtain the 4.1 line. **b** CaMV 35S::*AtPrx34* overexpression construct used to obtain the 30.2 line. **c** CaMV 35S::*GFP* construct for the localization of GFP alone. **d** CaMV 35S::*AtPrx33/34-GFP* constructs for cellular localization of the peroxidases. (e) *AtPrx33/34* endogenous promoter::*AtPrx33/34-GFP* constructs for subcellular localization of the peroxidases



A third construct used as control has been obtained by cloning 35S::*GFP-Term* in pCGN1547 (McBride and Summerfelt 1990).

The sequences of the individual primers are as follows (engineered restriction sites are underlined): *AtPrx33*, 5'-GGGGTACCGCTTGGTTTGGTTTCCATTG-3', 5'-GGGGTACCATGCAATTCTCTTCATCTTC-3' and 5'-CCGTTCTCGAGACATAGAACTTACAAAGTC-3' and *AtPrx34*, 5'-CCCAAGCTTTGGATTCTTC-3', 5'-CCGCTCGAGATGCATTTCTCTTCGTCTT-3' and 5'-CATGCCATGGGCATAGAGCTAACAAAGTC-3'. For the GFP analysis, seedlings were counterstained with 10 µg/ml propidium iodide and placed on slides in a drop of water. The GFP fluorescence was imaged with an Axioplan2 Zeiss microscope with narrow band excitation (470 ± 20 nm) and emission (510 ± 20 nm) filters (Chroma Technology Corp, VT, USA) and using the Metamorph software (Molecular Devices Corp, CA, USA).

#### Overexpression of *Atprx34* and RNAi constructs

For the overexpression experiment, *AtPrx34* cDNA sequence under the control of CaMV 35S (Fig. 1b) was cloned in pCHF3 vector using *KpnI* and *BamHI*. From the transgenic plants that have been obtained, only the line “30.2” has been used for an extensive phenotype study.

The RNAi construct with the whole *AtPrx34* cDNA (Fig. 1a) has been obtained in three successive steps in pBluescript KS+. The cDNA has been cloned in the antisense orientation with *EcoRI* and *BamHI*. A linker of 700 bp has been cloned into the previous plasmid with *HindIII* and *XhoI*. The final *43xrPtA-linker-AtPrx34* construct has been obtained by a three-way ligation: the *43xrPtA-linker* opened with *XbaI* and *XhoI* and the *AtPrx34* opened with *XhoI* and *PstI* was subcloned into pCHF5 with *XbaI* and *PstI*. The capacity of

the construct to form a hairpin loop has been controlled before plant transformation using an exonuclease after denaturation and quick renaturation. The construct was used to transform the *atprx33* insertion knock-out mutant, thus resulting in a double-transgenic line called “4.1”.

Complementation assays have been performed by transforming *atprx33* T-DNA mutant with the *AtPrx33::AtPrx33-GFP-Term* construct. Root and root cell lengths were determined in homozygous complemented lines. RT PCR using specific primers spanning the junction site *Atprx33-GFP* verified the level of *AtPrx33* transcript.

#### Plant transformation

All plasmids were introduced into *Arabidopsis* Col ecotype (except 4.1 double mutant in Ws) by *Agrobacterium tumefaciens*-mediated transformation using the spraying technique (Bent 2000). *Agrobacterium tumefaciens* strain ASE was used in all cases. The transformants were selected on ½ MS medium containing 50 µg/ml kanamycin or 40 µg/ml Basta, depending on the binary vector used. The presence of the transgenes in all transgenic plants was confirmed by genomic PCR using primers specific in each case.

#### Root and cell length measurements

The length of the roots and cells was measured on one-week old seedlings grown in square boxes placed in vertical position. Root length was measured on 40–50 seedlings from several independent batches. Cell length was determined by measuring 200 cells in the root hair zone from six independent seedlings. For this purpose, roots were stained with 10<sup>-4</sup> M DAPI and observed at a 10× magnification by fluorescence with an Axioplan2

Zeiss microscope (excitation:  $359 \pm 50$  nm, emission:  $460 \pm 50$  nm), using the Metamorph software for measurement. Differences between wild-type and transgenic seedlings were evaluated for every measurement assay using a 1-way between subjects ANOVA test (Analyse-it Software, v.1.71).

### Reverse transcriptase PCR

Reverse transcriptase-PCR was used as a semiquantitative method to assess the expression of peroxidase genes. Leaves, stems, flowers, and roots from 5-week old plants were harvested and frozen immediately in liquid nitrogen. Approximately, 100 mg of tissue sample was ground in liquid nitrogen, and total RNA was extracted with the Tri-reagent solution (Sigma) according to the instructions of the manufacturer. After quantification of the concentration by spectrophotometry and confirmation by electrophoresis, 1  $\mu$ g of the crude RNA preparations was treated with one unit of RNase-free DNase I (Promega). The DNA-free RNA was then used as a template during reverse transcription according to the ImPromII RT protocol from Promega. PCR amplification was conducted for up to 40 cycles using the following thermal profile: denaturation at 95°C for 1 min, annealing at 55°C for 1 min, and polymerization at 72°C for 30 s, with a 10 min terminal extension step at 72°C. To determine whether comparable amounts of RNA from the different tissues had been used for RT-PCR, the level of *AtPrx42* transcript was used as a constitutive control. Indeed, *AtPrx42* is strongly expressed in all *Arabidopsis* organs (Tognolli et al. 2002; Valério et al. 2004), it is the most abundant peroxidase in *Arabidopsis* (505 ESTs were found from a total of 353 000 ESTs indexed in TIGR) and its expression was found strong and stable independently of the age of the plants, various treatments and growth conditions in reverse transcription assays (data not shown). Reactions without RT were used to rule out contamination by genomic DNA. Primers used to determine the homozygosity have also been used for RT-PCR. The following primers were used for *AtPrx42* cDNA: 5'-GGTCCATCGTTTG-TACCCT-3' and 5'-CCCCTGTCTTTCTCACTTTT-3'.

Quantification of the RT-PCR bands on agarose was performed with the software QuantityOne (BioRad). The results shown in Fig. 4 represent the sum of four bands resulting from four independent experiments for each condition (light/dark).

### Expression in baculovirus-insect cell system and binding activity

The cDNA sequences encoding AtPrx33, AtPrx34 and AtPrx37 without the signal peptide have been cloned, respectively, with *Bam*HI/*Pst*I, *Bam*HI/*Eco*RI, and *Bam*HI/*Xba*I into pVL1392 vector (Pharminggen, San Diego, CA, USA) and expressed in baculovirus-insect

cells (Carpin et al. 2001). After purification, the resulting recombinant proteins were tested for their binding capacities. The binding of peroxidases to the  $\text{Ca}^{2+}$ -pectate gel was assessed by centrifugation as already described (Penel and Greppin 1996). APRX, an anionic peroxidase from zucchini (Carpin et al. 2001) and AtPrx32 from *Arabidopsis* (Dunand et al. 2002) have been used as positive controls. A horse-radish peroxidase mixture containing mainly the HRPC isoform (Fluka, Buchs, Switzerland) was used as a negative control for the binding activity. The assays were performed in a total volume of 100  $\mu$ l containing the same level of guaiacol peroxidase activity (0.025 OD<sub>470nm</sub>/min).

### Sequence analysis

The 1,000-bp region upstream each peroxidase gene was analyzed using PLACE and PlantCARE softwares (<http://www.dna.affrc.go.jp/htdocs/PLACE> and [oberon.rug.ac.be:8080/PlantCARE](http://oberon.rug.ac.be:8080/PlantCARE)).

## Results

### Identification of the *atprx33* and *atprx34* T-DNA tagged mutants

To obtain plant lines with a disruption in the *AtPrx33* and *AtPrx34* genes, we screened the collection of T-DNA insertion mutants of Feldmann (Feldmann et al. 1991) and the TAIR knockout facility (<http://www.arabidopsis.org>). We used a PCR strategy with primers specific for T-DNA borders and gene-specific sequence in order to identify T-DNA mutants for *AtPrx33* or *AtPrx34* genes. A homozygous line with insertions in intron 1 was obtained in the case of *atprx33*, leading to gene disruption 660 bp downstream of the ATG initiation codons (Fig. 2). A homozygous line with insertion 200 bp upstream of the ATG initiation codons was obtained for *atprx34* (Fig. 2). The position of the insert was verified using T-DNA specific primers, the wild-types (Col and Ws) being used as negative control. The homozygosity was confirmed by PCR with gene-specific primers flanking the T-DNA insert. No amplification was observed for the T-DNA mutants (Fig. 3a). The presence of a single insert and the homozygosity were confirmed with the ratio of resistant plants for both lines (data not shown).

Reverse transcription-PCR experiments on RNA from *atprx33* seedlings indicated the absence of transcripts from this gene in the mutant background, whereas amplification products were readily detectable in the wild-type seedlings (Fig. 3b). *Atprx34* transcripts could be slightly detected in the *atprx34* mutant, but their level was decreased when compared to the wild-type level in 2-week-old seedlings (Fig. 3c). This means that the transcription of *AtPrx34* was not completely

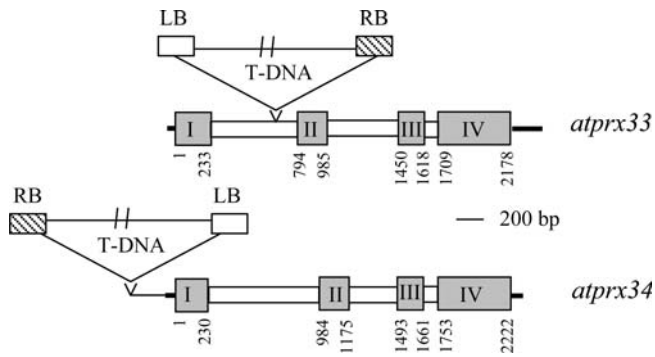


**Fig. 2** *AtPrx33* (M58380) and *AtPrx34* (X71794) gene structures and insertion sites of the T-DNA. Grey boxes represent exons and empty boxes introns (numbered from I to IV); bold lines are the predicted and observed 5' and 3'UTR. RB right border, LB left border

abolished by the presence of the insert in the promoter region.

### Expression profile of *AtPrx33* and *AtPrx34* peroxidase genes

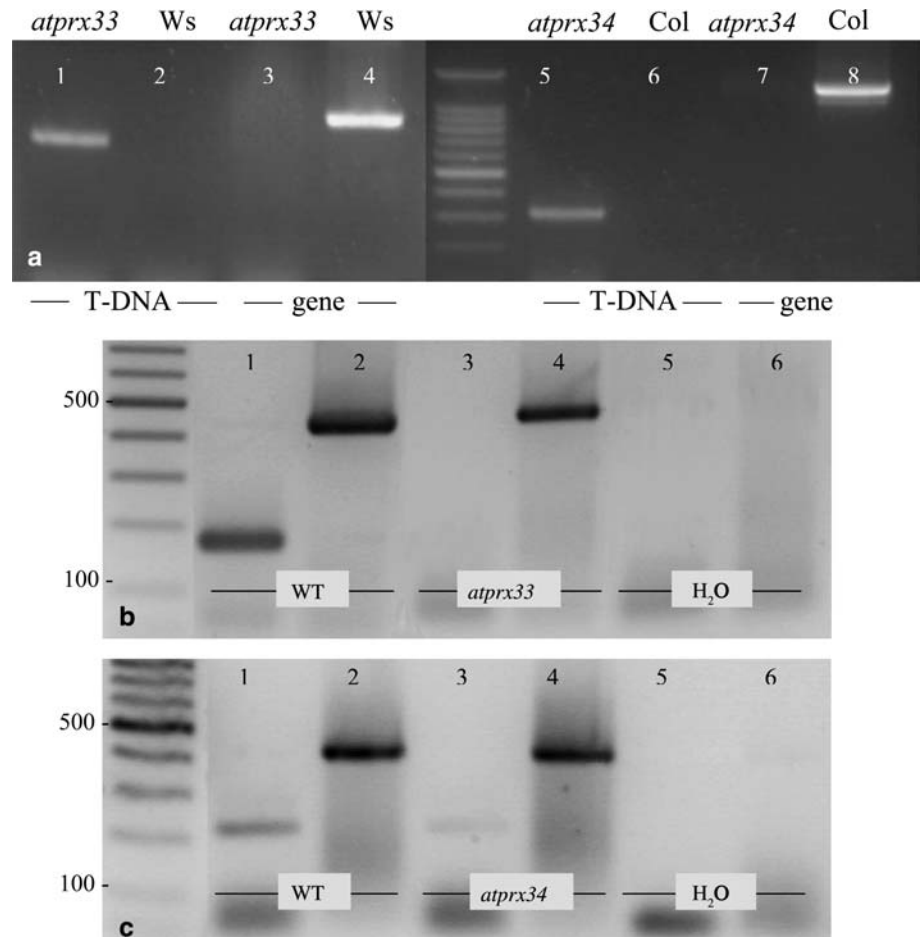
High level of *AtPrx33* transcripts was detectable in the roots of 5-week-old plants and at a lower extent in leaves

and stems. Some transcripts were also found in flowers. In contrast, low levels of *AtPrx34* transcripts were detected only in roots (Fig. 4a). *AtPrx33* transcripts increased with the age of seedlings, both in light and in the dark (Fig. 4b). *AtPrx34* transcripts, present at a much lower level seemed to increase as well. The expression of *AtPrx33* was largely lower in the dark than under light (Fig. 4b). In all cases, independently of the organs, the light quantity and the age of the plants, *AtPrx33* transcripts were more abundant than *AtPrx34* ones. The equivalent efficiency of *AtPrx33* and *AtPrx34* primer annealing was verified with genomic templates (data not shown).

### Subcellular localization of the *AtPrx33* and *AtPrx34* in planta

Plants were transformed with *Atprx33-GFP* and *Atprx34-GFP* constructs under the control of the CaMV 35S promoter. Endogenous promoters were also used, but in that case the expression was too low and the fluorescence could not be observed. Under the control of CaMV 35S, *AtPrx33-GFP*, and *AtPrx34-GFP* fusion proteins accumulated in cell walls (Fig. 5c-g). GFP protein alone had a nuclear and cytoplasmic localization

**Fig. 3** Molecular characterization of the *atprx33* and *atprx34* T-DNA tagged mutants. **a** Control of the position and homozygosity of the insert. Genomic DNA from *atprx33* and *atprx34* mutants and from the corresponding wild-types (Ws and Col, respectively) was used for PCR amplification with primers specific for the T-DNA insert or for the peroxidase genes. **b** *AtPrx33* transcript levels in 2-week-old *atprx33* and wild-type (WT) seedlings. RT-PCR with *AtPrx33* gene-specific primers (lanes 1, 3 and 5); with *AtPrx42* primers (lanes 2, 4 and 6). **c** *AtPrx34* transcript levels in 2-week old *atprx34* and wild-type seedlings. RT-PCR with *AtPrx34* gene-specific primers (lanes 1, 3 and 5); with *AtPrx42* primers (lanes 2, 4, and 6). RT-PCR products shown for *AtPrx33* and *AtPrx34* were amplified for 40 cycles from 1 µg of total RNA. In b and c, the *AtPrx42* transcript level was used as a constitutive control



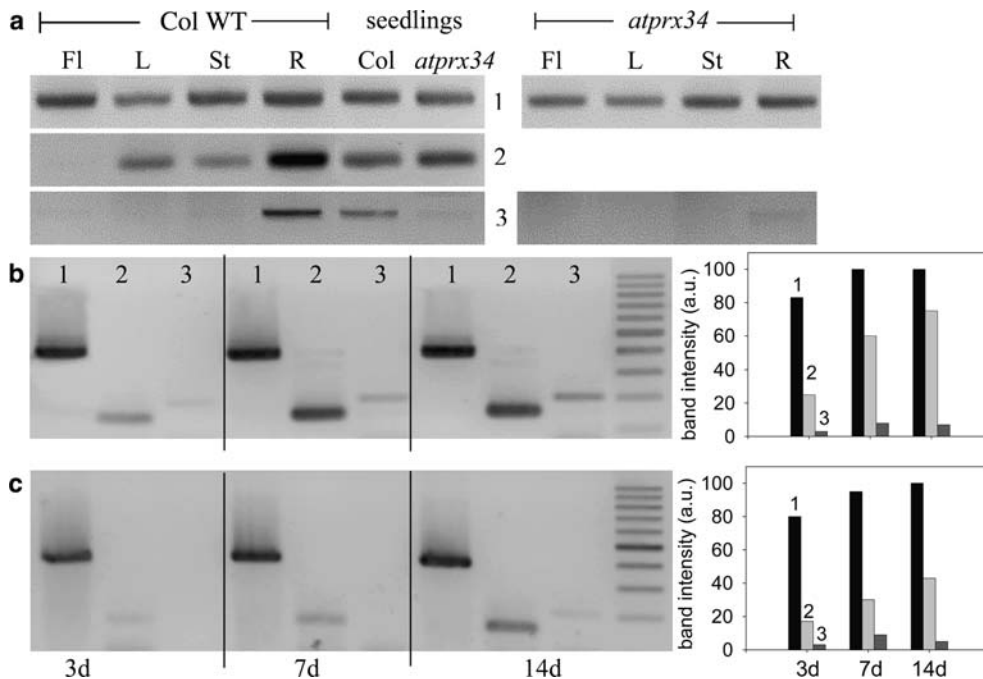


**Fig. 4** Expression level of *AtPrx42* (1), *AtPrx33* (2), and *AtPrx34* (3) genes assessed by RT-PCR. **a** Flowers (Fl), stems (St), and roots (R) from 5-week-old plants; 7-day-old whole seedlings from Columbia wild-type (Col), and *atprx34* mutant. **b** Columbia seedlings grown for 3, 7, and 14 days under a 16 h photoperiod. **c** Columbia seedlings grown for 3, 7, and 14 days in

darkness. In **b** and **c**, a representative gel and a graph corresponding to the mean of four independent experiments are shown. Total RNA (1  $\mu$ g) was used for RT-PCR with primers specific for *AtPrx42* (1), *AtPrx33* (2), and *AtPrx34* (3) genes. The RT-PCR products shown were amplified for 40 cycles. The *AtPrx42* transcript level was used as a constitutive control

(von Arnim et al. 1998) (Fig. 5a, b). In vitro, recombinant *AtPrx33*, *AtPrx34*, and *AtPrx37*, produced by the baculovirus insect cell system, showed some capacity to bind to the  $\text{Ca}^{2+}$ -pectate complex, which is mainly found in the middle lamella. Their binding activities were much lower than the binding capacity of *AtPrx32* and zucchini APRX, but significant when compared to the lack of binding of horseradish peroxidase (Fig. 6). *AtPrx32* and HRPC both show high homology at the protein level with *AtPrx33/34* (over 87%), but only the former bears the putative pectate binding domain.

#### Root length and peroxidase gene expression

The length of roots was measured on various transgenic seedlings, including *atprx33*, *atprx34*, the *AtPrx34* overexpressor 30.2, and the 4.1 RNAi double mutants. Since the mutants were obtained in two different backgrounds, Columbia and Wassilewskija *Arabidopsis* were also analyzed. The 4.1 double mutants do not contain *AtPrx33* transcripts and exhibit a reduction of *AtPrx34* mRNA (Fig. 7a). Seedlings containing a T-DNA inserted in the *AtPrx34* promoter sequence (*atprx34*) showed a reduced expression of *AtPrx34* and the seedlings containing the 35S::*AtPrx34* construct (30.2 line) an accumulation of *AtPrx34*. *atprx34*

seedlings had no significant root length variation when compared to the wild-type plants, whereas the 30.2 mutant had clearly longer roots (Fig. 7b). In knocked-out *atprx33* plants and in the double mutant (4.1 line), a significant reduction of the root length could be observed (Fig. 7b). The root length reduction is additive when both genes are affected. The fully elongated cells present in the root hair zone were also measured. It appeared that the length of these cells was also significantly reduced in *atprx33* and 4.1 mutants and increased in 30.2 mutant.

In order to determine the heritability of the mutation in mutant lines, homozygous transgenic plants were crossed with corresponding wild-type ecotypes. The F1 (for overexpressor lines) and the F2 progenies (for the *atprx33* mutant) showed the appropriate root phenotype (data not shown). The co-segregation of the resistance and of the phenotype confirmed that the mutations related to *AtPrx33* and *AtPrx34* are directly responsible for the modification of the root length.

Finally, complementation assays were performed by introducing the *AtPrx33::AtPrxP33-GFP-Term* construct in knocked-out *atprx33* plants. A significant increase of root and root cell lengths was observed and compared to *atprx33* plants in a complemented line. There was no significant difference between this complemented line and the Ws wild-type control (Fig. 8).

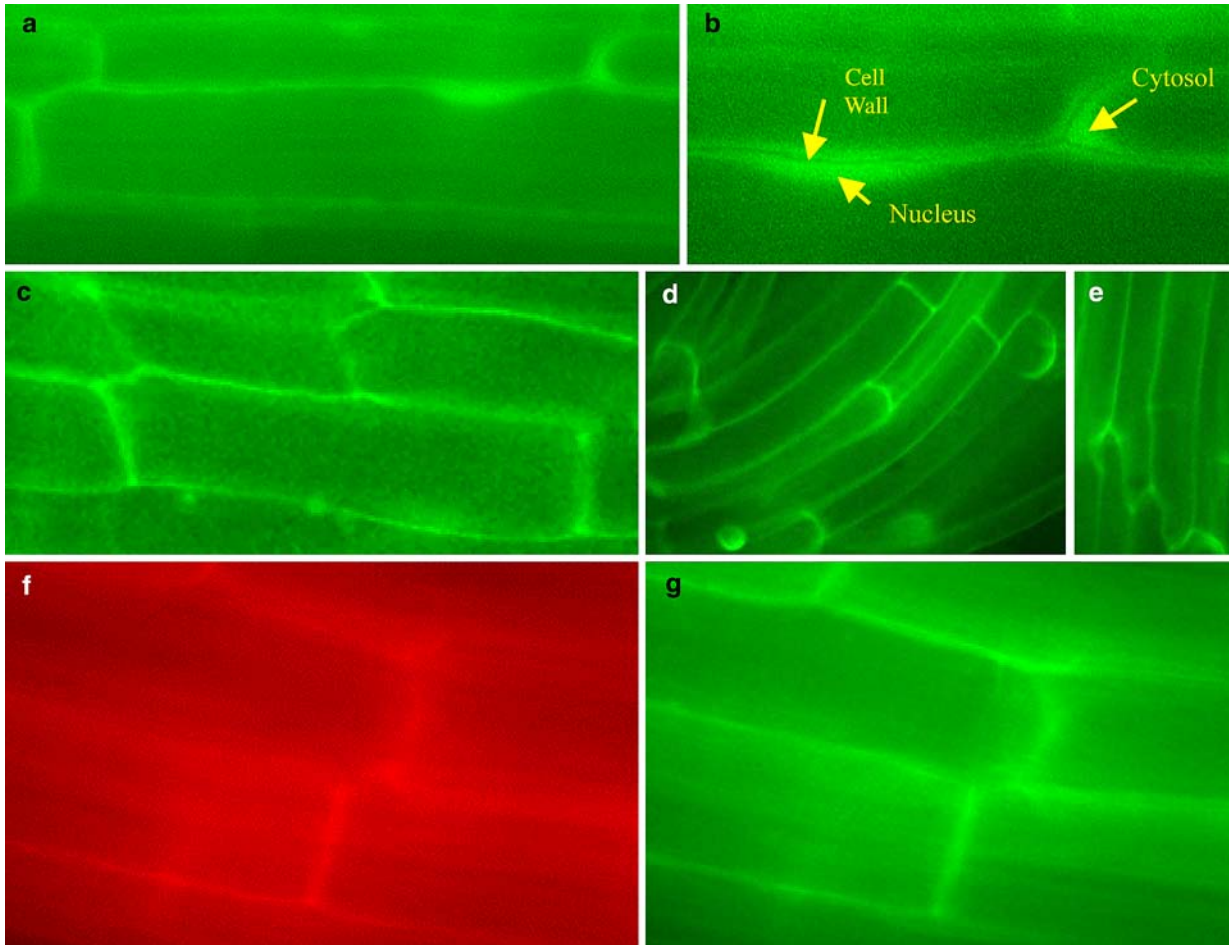


**Fig. 5** Detection of GFP fluorescence in roots of seedlings transformed with a CaMV 35S::GFP construct (a, b), with a CaMV 35S::*AtPrx33*-GFP construct (c–e) and with a CaMV

35S::*AtPrx34*-GFP construct (f, g). Staining with 10 µg/ml propidium iodide (f). Cell wall (unstained zone), nucleus, and cytosol (stained zones) are indicated by arrows in B

## Discussion

### Analysis of the nucleotide sequences

The structure of *AtPrx33* and *AtPrx34* corresponds to a classical peroxidase gene with three introns and four exons (Tognolli et al. 2002). The first 100 bp upstream

the ATG codon of the two genes are highly conserved. This short sequence contains the TATA box and is sufficient for a basal expression, but probably does not allow a fine and specific regulation of expression as shown by T-DNA insertion in the *AtPrx34* promoter. Indeed, the insertion 200 bp upstream of the ATG should remove light response and root localization. Known cis-elements found in the promoter of *AtPrx33*

**Fig. 6** Binding of recombinant peroxidases to  $\text{Ca}^{2+}$ -pectate. The assays were performed in the presence of 10 µg of polygalacturonic acid and 2 mM  $\text{CaCl}_2$  in a total volume of 100 µl with the same level of peroxidase activity (Penel and Greppin 1996). After centrifugation, the peroxidase activity was measured in the  $\text{Ca}^{2+}$ -pectate pellets (○) and in the corresponding supernatant (◐). The data are the means of three independent experiments  $\pm$  SD

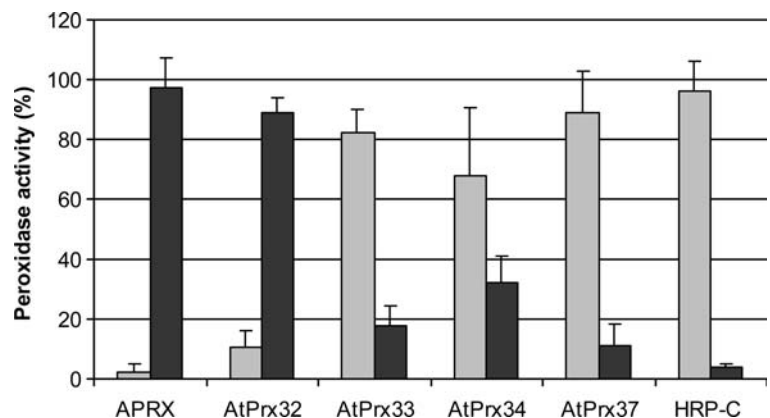
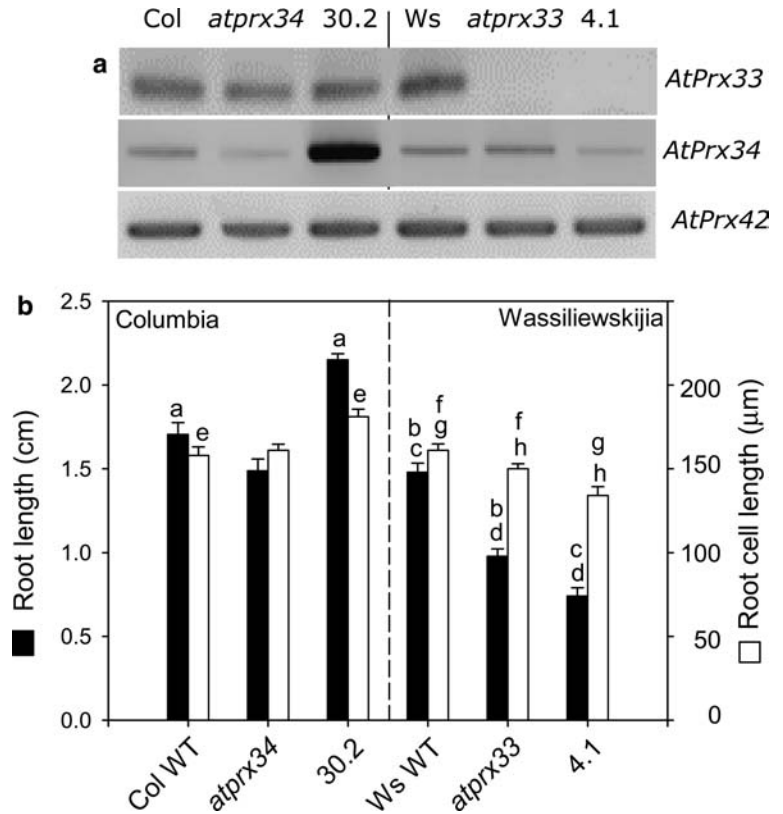


**Fig. 7** Expression of *AtPrx33*, *AtPrx34* and *AtPrx42* genes and the measurement of root length and cell root length in various transgenic *Arabidopsis* seedlings. **a** Expression of the three peroxidase genes in *apr34* and overexpressor 30.2 mutants in a Columbia (Col) background and in *atprx33* and RNAi 4.1 mutants in a Wassilewskija (Ws) background, assessed by RT-PCR. The *AtPrx42* transcript level was used as a constitutive control in the various seedlings. **b** Root lengths and cell root lengths of 7-day-old seedlings from the plant lines described in a. The differences between wild-type and corresponding mutant seedlings were analyzed by 1-way ANOVA test. Same letters indicate significant differences with *P* values: *P* < 0.0001 (a,b,c,g); *P* = 0.0046 (d); *P* = 0.001 (e); *P* = 0.0297 (f); *P* = 0.0121 (h)



and *Atprx34* genes have been listed in Table. 1. There is a similar distribution of cis-elements related to the control by light and the expression in root. This *in silico* analysis is in agreement with the actual expression pattern, which showed a preferential transcription in the

roots and an up-regulation by light (Fig. 4). In contrast, large differences exist for the abscissic acid response elements (seven elements in *AtPrx33* and none in *AtPrx34*) and for the salicylic acid response elements (six elements in *AtPrx34* and none in *AtPrx33*), which is in line with the idea of a similar activity but a different regulation for the two peroxidases.

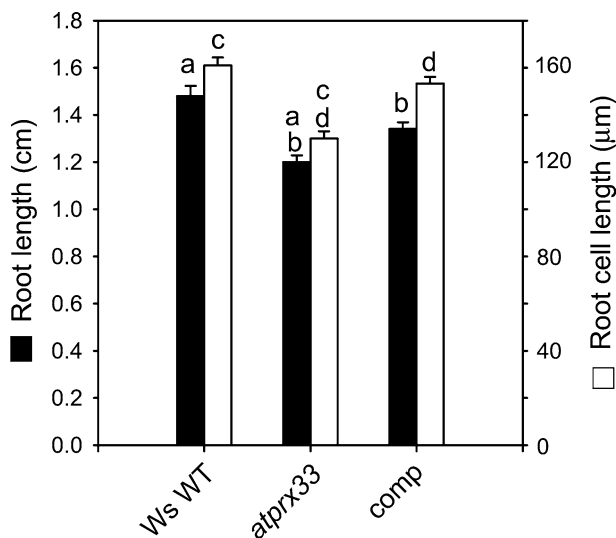


**Fig. 8** Complementation assays. Root and cell root lengths were determined for 7-day-old seedlings from Wassilewskija (Ws), *atprx33* and *atprx33* complemented line (comp). The differences between the seedlings were analyzed by a 1-way ANOVA test. Same letters indicate significant differences with *P* values: *P* < 0.0001 (a, c, d); *P* = 0.0007 (b)

*AtPrx33* and *AtPrx34* are cell wall associated and involved in cell elongation

*AtPrx33* and *AtPrx34* are members of a same gene cluster and show a high level of homology with 90% of identity. Both peroxidases are localized in cell walls (Fig. 5). They have an amino acid motif including three lysine residues, which is similar to the well-characterized  $\text{Ca}^{2+}$ -pectate binding site of the zucchini peroxidase APRX (Carpin et al. 1999, 2001; Dunand et al. 2002). Purified *AtPrx34* has also been shown to bind to  $\text{Ca}^{2+}$ -pectate (Shah et al. 2004) and recombinant *AtPrx33* and *AtPrx34* produced by insect cells exhibited some affinity for  $\text{Ca}^{2+}$ -pectate (Fig. 6). This means that, their localization within the cell walls could be modulated by  $\text{Ca}^{2+}$ , as already demonstrated for APRX (Carpin, 2001).

*AtPrx33* and *AtPrx34* sequences possess a signal peptide and a C-terminal extension. The signal peptide targets the protein to endoplasmic reticulum and the secretory pathway, whereas the C-term extension (CTPP) may address the protein to the vacuole

**Table 1** Main *cis*-elements present in the 1,000 bp upstream the *AtPrx33* and *AtPrx34* genes

Motif	Sequence	Function	Position for <i>AtPrx33</i>	Position for <i>AtPrx34</i>
ABRE	<u>YACGTGGC</u>	Abscissic acid responsiveness	<u>46(-), 47, 144(-), 222(-), 539(-), 540, 898(-)</u>	
ARF/AuxREs	TGTCTC	Auxin response element	618(-)	247(-)
AuxRR	GGTCCAT	Auxin response	938(-)	
ERE	ATTTCAaa	Ethylene-responsive element	647	5, 295, 337
G-box	CACGTG	Element involved in light responsiveness	45, 538	
GA-motif	<u>ATAGATAA</u>	Part of a light responsive element	273(-), <u>477(-)</u>	725
GATA-box	<u>GATAGa</u>	Part of a light responsive element	65(-), <u>652</u>	244 (-), 636, 790
LAMP-element	CTTTATCA	Part of a light responsive element		303
LTR	CCGAaa	Low-temperature responsiveness	616, 76(-)	585
MBS	CAACTG	MYB binding site involved in drought-inducibility	247(-)	
P-box	CCTTTTG	Gibberellin responsive element		833(-)
Root motif	ATATT	Root localization	289(-), 407(-), 410, 645, 791(-), 792, 852	6(-), 406(-), 407, 518(-), 522, 561, 616, 644(-)
TGA-element	AACGAC	Auxin response element	808	
W-box	<u>TTGACC</u>	Salicylic acid responsiveness	903	<u>378(-), 579, 672(-), 813, 903, 979</u>

The data have been obtained with PlantCare and PLACE. Indicated positions are relative to the ATG codon. Underlined positions correspond to the underlined part of the *cis*-element

(Neuhaus 1996). However, a recent study cast some doubt on the validity of this hypothesis in the case of a horseradish peroxidase (Kis et al. 2004), and so far there has been no evidence suggesting that the CTPP is cleaved from HRPc1a for the cell wall targeting (Matsui et al. 2003). Similarly to APRX, which also has a C-term extension but was found in apoplast (Carpin et al. 1999), *AtPrx33* and *AtPrx34* are localized in the cell wall (Fig. 5). Even if both proteins transit via the vacuole (Carter et al. 2004), they finally end in the apoplast. The same transitory targeting has been observed for a cell-wall-associated kinase 1 (WAK1) found in the vacuole (Carter et al. 2004) but known to bind the Ca<sup>2+</sup>-pectate complex (Decreux and Messiaen 2005). All WAK family members (WAK1–5) exhibit a similar protein length without apparent C-term extension. Thus, vacuole targeting could be transient before a final localization in the cell wall regulated by the presence of the CTPP but not related to the cleavage of this extension. Regarding *AtPrx33/34* GFP fusion protein, substantial evidence shows that the fusion proteins are correctly folded and active: GFP fluorescence was detected in the plants containing *AtPrx33/34*-GFP, and the *AtPrx33*-GFP construct can complement the *atprx33* mutant phenotype.

The peroxidase cellular localization could be associated with a particular activity in relation to cell wall elongation. *AtPrx33* and *AtPrx34* are highly homologous and most likely have similar enzymatic properties in the cell wall. On the other hand, we have observed important difference concerning the transcription profile. These variations might explain the presence of two very close isoforms, performing similar tasks, but differentially transcribed in response to various stimuli.

Knocking out *AtPrx33* gene expression resulted in the reduction of root elongation. However, this did not correspond with a significant modification of the total

peroxidase activity (data not shown). The high number of peroxidase isoforms present in Arabidopsis can easily explain this. Even if the overall peroxidase activity was not affected in *atprx33* or 4.1 mutants, the *AtPrx33* protein was most likely absent since there were no detectable transcripts. This absence resulted in a reduction of growth, thus suggesting that this peroxidase is involved in growth promoting reactions. This was confirmed by the additional growth reduction observed following *AtPrx34* downregulation in 4.1 double mutant, the restoration of normal root growth in *atprx33* mutant complemented with *Atprx33::Atprx33-GFP* construct and the stimulation of root growth brought about in the 30.2 mutant overexpressing *AtPrx34*. Another peroxidase, horseradish prxC1a peroxidase, was already reported to stimulate growth when expressed in hybrid aspen (Kawaoka et al. 2003). In the present work, there was a correlation between the root length and the length of root cells (Fig. 7), suggesting that the observed modifications of root growth are due to the changes in cell elongation. This means that *AtPrx33* and *AtPrx34* would be involved in reactions promoting cell elongation, for example free radical production that may loosen cell wall, as proposed by Schopfer (2001). The level of *AtPrx33* and *AtPrx34* transcripts was light- and age-dependent (Fig. 4), which can be related to the stimulating effect of light and of the stage of development on root growth. The light regulation of both genes is also in line with the presence of numerous light related elements in their promoter sequences (Table 1), and with observations reporting a phytochrome-dependent regulation of peroxidases in other plant species (Kim et al. 1989; Casal et al. 1994).

The assessment of the transcript levels by RT-PCR indicated that *AtPrx33* gene was expressed at a much higher rate than *AtPrx34*. This is not in agreement with a previous northern blot analysis (Shah et al. 2004). This

latter discrepancy could be explained by the specificity of the primers used for the PCR amplification versus the lower specificity of the cDNA probes used previously for the northern blot analysis. However, both techniques showed that *AtPrx33* and *Atprx34* mRNAs accumulated mainly in roots. Concerning the EST counts, it is probable that the developmental stage at which we studied our plants was not one in which *AtPrx34* expression was the highest. Further studies are needed to clarify this point.

The results obtained in this work as well as the presence of auxin related cis-elements in the promoter region of *AtPrx33* and *Atprx34* genes (Table 1) argue in favor of an active role of the two encoded peroxidases in root cell elongation.

**Acknowledgements** We thank Prof. Susan Gasser (Friedrich Miescher Institute, FMI, Basel, Switzerland) for the use of the Zeiss Axioplan II microscope, Dr. Thierry Laroche (FMI) for his scientific comments and technical support, and Prof. Christian Fankhauser (University of Lausanne, Switzerland) for the gift of the binary vectors pCHF3 and pCHF5. This work was supported by the Swiss National Science Foundation (grant 31-068003.02).

## References

- Alonso JM, Stepanova AN, Leisse TJ, Kim CJ, Chen H, Shinn P, Stevenson DK, Zimmerman J, Barajas P, Cheuk R, Gadrinab C, Heller C, Jeske A, Koesema E, Meyers CC, Parker H, Prednis L, Ansari Y, Choy N, Deen H, Geralt M, Hazari N, Hom E, Karnes M, Mulholland C, Ndubaku R, Schmidt I, Guzman P, Aguilar-Henonin L, Schmid M, Weigel D, Carter DE, Marchand T, Risseuw E, Brogden D, Zeko A, Crosby WL, Berry CC, Ecker JR (2003) Genome-wide insertional mutagenesis of *Arabidopsis thaliana*. *Science* 301:653–657
- Bent AF (2000) *Arabidopsis* in planta transformation. Uses, mechanisms, and prospects for transformation of other species. *Plant Physiol* 124:1540–1547
- Carpin S, Crevecoeur M, de Meyer M, Simon P, Greppin H, Penel C (2001) Identification of a  $\text{Ca}^{2+}$ -pectate binding site on an apoplastic peroxidase. *Plant Cell* 13:511–520
- Carpin S, Crevecoeur M, Greppin H, Penel C (1999) Molecular cloning and tissue-specific expression of an anionic peroxidase in zucchini. *Plant Physiol* 120:799–810
- Carter C, Pan S, Zouhar J, Avila EL, Girke T, Raikhel NV (2004) The vegetative vacuole proteome of *Arabidopsis thaliana* reveals predicted and unexpected proteins. *Plant Cell* 16:3285–3303
- Casal JJ, Mella RA, Ballare CL, Maldonado S (1994) Phytochrome-mediated effects on extracellular peroxidase activity, lignin content and bending resistance in etiolated *Vicia faba* epicotyls. *Physiol Plant* 92:555–562
- Decreux A, Messiaen J (2005) Wall-associated kinase WAK1 interacts with cell wall pectins in a calcium-induced conformation. *Plant Cell Physiol* 46:268–278
- Dunand C, Tognolli M, Overney S, von Tobel L, De Meyer M, Simon P, Penel C (2002) Identification and characterisation of  $\text{Ca}^{2+}$ -pectate binding peroxidases in *Arabidopsis thaliana*. *J Plant Physiol* 159:1165–1171
- Feldmann KA, Wierzbicki AM, Reiter RS, Coomber SA (1991) T-DNA insertion in *Arabidopsis*. In: Hermann R, Larkins B (eds) *Plant molecular biology*. Plenum Press, pp 563–574
- Gajhede M, Schuller DJ, Henriksen A, Smith AT, Poulos TL (1997) Crystal structure of horseradish peroxidase C at 2.15 Å resolution. *Nat Struct Biol* 4:1032–1038
- Gaspar T, Kevers C, Penel C, Greppin H, Reid D, Thorpe T (1996) Plant hormones and plant growth regulators in plant tissue culture. *In Vitro Cell Dev-Plants* 32:272–289
- Hajdukiewicz P, Svab Z, Maliga P (1994) The small, versatile pPZP family of *Agrobacterium* binary vectors for plant transformation. *Plant Mol Biol* 25:989–994
- Kawaoka A, Matsunaga E, Endo S, Kondo S, Yoshida K, Shimmyo A, Ebinuma H (2003) Ectopic expression of a horseradish peroxidase enhances growth rate and increases oxidative stress resistance in hybrid aspen. *Plant Physiol* 132:1177–1185
- Kim SH, Shinkle JR, Roux SJ (1989) Phytochrome induces changes in the immunodetectable level of a wall peroxidase that precede growth changes in maize seedlings. *Proc Natl Acad Sci USA* 86:9866–9870
- Kis M, Burbridge E, Brock IW, Heggie L, Dix PJ, Kavanagh TA (2004) An N-terminal peptide extension results in efficient expression, but not secretion, of a synthetic horseradish peroxidase gene in transgenic tobacco. *Ann Bot (Lond)* 93:303–310
- Matsui T, Nakayama H, Yoshida K, Shimmyo A (2003) Vesicular transport route of horseradish C1a peroxidase is regulated by N- and C-terminal propeptides in tobacco cells. *Appl Microbiol Biotechnol* 62:517–522
- McBride KE, Summerfelt KR (1990) Improved binary vectors for *Agrobacterium*-mediated plant transformation. *Plant Mol Biol* 14:269–276
- Murashige T, Skoog F (1962) A revised medium for rapid growth and bioassays with tobacco tissue cultures. *Physiol Plant* 15:473–497
- Neuhaus JM (1996) Protein targeting to the plant vacuole. *Plant Physiol Biochem* 34: 217–221
- Passardi F, Cosio C, Penel C, Dunand C (2005) Peroxidases have more functions than a Swiss army knife. *Plant Cell Rep* 24:255–265
- Passardi F, Penel C, Dunand C (2004) Performing the paradoxical: how plant peroxidases modify the cell wall. *Trends Plant Sci* 9:534–540
- Penel C, Greppin H (1996) Pectin binding proteins: characterization of the binding and comparison with heparin. *Plant Physiol Biochem* 34:479–488
- Savitsky PA, Gazaryan IG, Tishkov VI, Lagrimini LM, Ruzgas T, Gorton L (1999) Oxidation of indole-3-acetic acid by dioxygen catalysed by plant peroxidases: specificity for the enzyme structure. *Biochem J* 340:579–583
- Schopfer P (2001) Hydroxyl radical-induced cell-wall loosening in vitro and in vivo: implications for the control of elongation growth. *Plant J* 28:679–688
- Shah K, Penel C, Gagnon J, Dunand C (2004) Purification and identification of a  $\text{Ca}^{2+}$ -pectate binding peroxidase from *Arabidopsis* leaves. *Phytochemistry* 65:307–312
- Tognolli M, Penel C, Greppin H, Simon P (2002) Analysis and expression of the class III peroxidase large gene family in *Arabidopsis thaliana*. *Gene* 288:129–138
- Valério L, De Meyer M, Penel C, Dunand C (2004) Expression analysis of the *Arabidopsis* peroxidase multigenic family. *Phytochemistry* 65:1331–1342
- von Arnim AG, Deng XW, Stacey MG (1998) Cloning vectors for the expression of green fluorescent protein fusion proteins in transgenic plants. *Gene* 221:35–43
- Welinder KG (1992) Superfamily of plant, fungal and bacterial peroxidases. *Curr Opin Struct Biol* 2:388–393